Analysis of Chest Injuries to Child Occupants Seated in Impact Shield CRS based on Dummy tests, FE Simulations and Animal Tests

Yong Han, Jun Ouyang, Koji Mizuno, Anguo Cang

Abstract The chest injury risk to a child occupant in a child restraint system (CRS) was investigated using Q3 dummy tests, finite element (FE) simulations (Q3 dummy and human models) and animal tests. The investigation was done for two types of CRSs (impact shield CRS and five-point harness CRS), based on the UN R44 dynamic test. The tests using a Q3 dummy indicated that although the chest deflection in the impact shield was large, it was less than the injury threshold (40 mm). From the computational biomechanics simulations (using finite element FE analysis), it was predicted that the Q3 dummy chest is loaded by the shield and deforms appreciably under this load. On the other hand, the deformation of the shield was small. To clarify whether internal organ injuries due to chest compression can occur for an impact shield and a five-point harness CRS, four experiments were performed using Tibetan miniature pigs with weights ranging from 11 kg to 13 kg. Severe internal organ injuries (lung contusion, coronary artery laceration, liver laceration) were found for the CSR with an impact shield. It is concluded that it is likely that the internal organ injuries without rib fractures could occur to child occupants sitting in the CRS equipped with an impact shield.

Keywords Animal test, child occupant safety, impact shield CRS, inner organ injuries, Q3 dummy test.

I. INTRODUCTION

Accident data have demonstrated that a child restraint system (CRS) is effective for preventing injuries to children [1-2]. There are three types of forward-facing CRS: five-point harness, impact shield, and booster seat with a three-point seat belt. Many studies have examined the differences in the biomechanical/mechanical responses and injury risk of child occupants for various restraints. Melvin and Weber, have shown from sled tests using CRSs that the kinematic behaviour of a child dummy depends on the CRS type in which it is seated [3]. By attaching an abdominal sensor, they showed that the geometry and stiffness of the shield could affect the torso flexion and abdominal pressure. Whitman *et al.* [4] investigated severe accidents involving children using a booster-with-shield restraint, and concluded that a lap-/shoulder-belt would be needed to control the upper torso restraint in order to prevent large head excursions and loads to the abdomen. Langwieder *et al.* [5] investigated the German accident data and found that the injury risks of children were lower in an impact shield CRS than in a four-/five-point harness CRS. However, sled tests using child dummies do not seem to confirm this low probability of injury observed for impact shield CRSs in accidents [6]. In an impact shield CRS, the chest of occupants is loaded directly by contact with the shield during impacts, and the chest deflection tends to be large. This is different for a five-point harness CRS where the rib cage and both shoulders are restrained by the shoulder harness and the pelvis is restrained by the lap harness. Thus, as the sternum is not directly loaded in five-point harness CRS, the chest deflection is small [7]. In the Japan New Car Assessment Program (JNCAP), CRSs have been tested using a Hybrid III 3-year-old (3YO) dummy placed in the ECE seat subjected to a velocity change of 55 km/h. The rib cage of the Hybrid III 3YO bottomed out and the sternum made contact with the spine box in some impact shield CRSs in the JNCAP tests. However, the commonly accepted injury threshold of the chest deflection for children has not been established yet, and the chest deflection in the impact shield CRS is not evaluated in JNCAP. Tanaka *et al.* [6] examined several types of impact shield CRS from the experiments and FE simulations. They indicated that the chest deflection can be affected by the shield geometry; the shield which supports the pelvis can mitigate the chest deflection.

Y. Han (e-mail: yonghan@xmut.edu.cn; tel: +86 592 629 1677) is an associate professor in vehicle engineering at Xiamen University of Technology, China. J. Ouyang is Professor in the Department of Human Anatomy at Southern Medical University, China. K. Mizuno is a professor in the Department of Mechanical Science & Engineering at Nagoya University, Japan. A.G. Cang is director of the Transport Restraint System laboratory of Guangdong Inspection and Quarantine Technology Center, China.

There are also concerns that small children might be ejected from impact shield CRS during vehicle rotations such as offset impact and roll over. The child torso is not restrained with a harness in the shell of an impact shield CRS, which means that children can be lifted up from the CRS cushion and can rotate around the shield. As a result, the child could be ejected from the CRS. This is an important issue for an impact shield CRS as one of the key roles of a CRS is to contain a child occupant within the CRS and prevent impact between the child occupant and vehicle interior. The Q3 dummy kinematic behaviour was examined in two rollover tests [8]. As the rolling of the vehicle progressed, the gap between the child occupant and the shield increased. Finally, the Q3 dummy was ejected from the impact shield CRS. Moreover, the trend of lift-up behaviour of the Q3 dummy was observed during the rebound phase for impact shield CRS in offset frontal impact tests in Euro NCAP [9].

In order to investigate injuries to children in various impact scenarios, a three-year-old (3YO) child human finite element (FE) model was developed by Mizuno *et al.* [7]. Taking the anthropometry and material properties of a 3YO child into account, the model was made by scaling the adult human finite element (FE) model THUMS (Total Human Model for Safety). The kinematic behaviour of this model was compared with that of the Hybrid III FE model for an impact shield CRS under the ECE R44 impact conditions. The results indicated that the torso of the child model bent around the shield due to the spine's flexibility. On the other hand, the Hybrid III 3YO dummy model has a very stiff spine box that rotated upward around the shield, and the pelvis of the Hybrid III model lifted-up from the CRS cushion. Zhang *et al.* [10] have obtained similar results for the Q3 dummy. They used a multi-body dynamics (implemented using Madymo) child model and the Q3 dummy multibody model for the impact shield CRS. The multi-body child model bent around the shield, whereas the pelvis of the Q3 dummy lifted up from the CRS cushion. They concluded that the lift-up behaviour is limited to mechanical dummies with a stiff spine box, and that such behaviour is not observed for child human models. They also added that there have been no reports of a child being ejected from the modern group I impact shield CRS in real-world accidents.

In the impact shield CRS, the shield supports the chest. Kent *et al.* [11] conducted adult cadaver tests with various chest restraints, and showed that the stiffness of the chest increases with the contact area between the restraint system and the chest. Moreover, they found that if the restraint system (such as a seatbelt) constrains the shoulder, the chest stiffness increases. In the impact shield CRS, the shoulders of the child are not constrained and the chest deflection can be large. In addition, for a child FE model seated in the impact shield CRS, it was observed that the chest was compressed substantially not only by the inertial compressive loading by the torso but also by the tensile loadings applied to the torso from the upper and lower extremity inertial force [7]. Thus, the chest deflection of child occupant can be potentially large for an impact shield CRS.

The rib cage of children has low stiffness and the organ injuries can occur before rib cage fractures are realized. Based on scaling from the chest deflection threshold (62 mm) of adult male in distributed loading, Mertz et al. [12] proposed the injury assessment reference value (IARV) of chest deflection of 35.8 mm as corresponding to a 5% risk of an AIS4+ organ injury for a 3YO child. The EEVC proposed several IARVs for Q3 chest deflection [13]. In their study, the chest deflection of adult male (50 mm) in UN R94 tests was scaled to 46.5 mm (AIS3+). Using the data from accident reconstructions, they determined the IARV for chest deflection at 38 mm for 20% risk and 48 mm for 50% risk of an AIS3+ injury using a certainty method. It was 36 mm and 53 mm for 20% risk and 50% risk of an AIS3+ injury, respectively, using a logistic method. As a pragmatic threshold, the Q3 chest deflection of 40 mm was proposed for amendments to R129 phase 1. (In phase 1 of R129, the chest deflection is monitored only.) [14]. This value (40 mm) is 33% of the chest depth (122 mm) of a 3YO child. For the UN R44 test, the chest deflection of the Q3 and Hybrid III 3YO dummy ranged from 30 mm to 57 mm [7]. Even though the chest deflection exceeded the proposed IARV, it is still not clear whether chest injuries occur since chest injuries to children are not observed frequently in real-world accidents. In forwarding facing (FF) CRS impacts, chest injuries account for 2.8% as compared to 56.9% for the head, 8.3% for the face, and 3.3% for the abdomen of the AIS 2+ injuries observed in accidents [15]. Because of the low injury risk to the chest, chest deflection is not included in the CRS regulations, such as FMVSS 213 and UN R129 phase 1.

Experiments and simulations in literatures have shown that the chest of the child occupant is substantially loaded in an impact shield CRS. However, accident data do not confirm that an impact shield CRS poses a high injury risk to children [5]. To determine whether the impact shield CRS has a potential to cause chest injuries to children, it needs to be determined whether the loading to the chest reaches internal organ injury threshold for children, even though rib fractures do not occur. To determine the chest loading, tests using Q3 dummy were conducted for impact shield CRSs according to UN R44. FE simulations were carried out to understand the interaction between the shield and the chest. Finally, Tibetan miniature pigs were seated in the impact shield CRS and subjected to sled impacts according to the UN R44 test protocol. Chest injuries to the pigs were examined in order to determine whether the internal organ injuries could occur without rib fractures due to the load induced by an impact shield CRS.

II. METHODS

Dummy Tests

Frontal impact tests using CRSs were conducted according to UN R44 except for using a Q3 dummy instead of using a P3 dummy. The sled velocity change was 50 km/h. Table I shows the test matrix. Two impact shield CRSs (CRS A, B) were tested; and one five-point harness CRS (CRS C) in a forward-facing (FF) condition was also conducted for comparison with the impact shield CRS tests. The key differences between CRS A and CRS B are: 1) The shield in CRS A covers the upper thorax of Q3 dummy, while the shield in CRS B covers the middle thorax of the Q3 dummy; 2) In CRS B, the pelvis of the Q3 dummy can be supported by the shield (see Fig.1); 3) In CRS A, the rear shape of the shield in the area of contact with the chest of Q3 dummy is relatively flat; whereas, in CRS B, the rear shape of the shield is concave and rounded and matches well the shape of the Q3 dummy chest.

The impact shield CRSs were installed in the ECE seat with a seatbelt and with an ISOFIX anchorage. The CRS B has a soft ISO connector which connects the CRS shell and the ISOFIX anchorage with the belt. The seatback of the impact shield CRS is designed to be locked so as not to push the back of a child occupant during a frontal impact. The Q3 dummy was placed in the CRS following the procedure prescribed in the UN R129 (Fig. 1). In order to see the geometric relationship between the shield and the ribcage, the jacket of the Q3 dummy was removed. The chest accelerations and deflections were compared for the three CRSs to investigate the loading on the chest. The sled acceleration is shown in Fig. 2.

TABLE I
Q3 DUMMY CRS SLED TEST MATRIX

Test No.	CRS model	Type	CRS installation
D001	CRS A	Impact shield	S/B, ISOFIX (hard)
D002	CRS B	Impact shield	S/B, ISOFIX (soft)
D003	CRS C FF	Five-point harness	ISOFIX (hard), Support leg

(a) CRS A (b) CRS B (c) CRS C FF

Fig. 1. CRS test set-up.

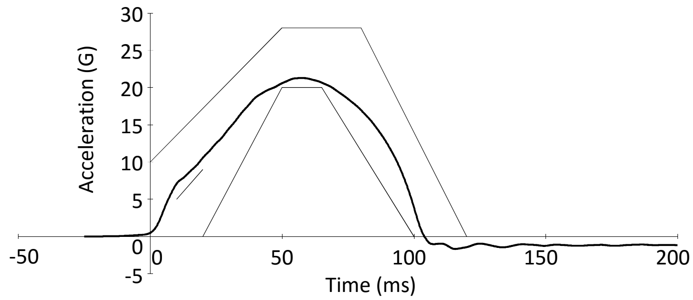

Fig. 2. Acceleration of the sled with ECE R44 corridor.

FE simulation

In this study, the protection performance of an impact shield CRS (CRS B) was analyzed using the Q3 dummy and THUMS 3YO finite element FE models in LS-DYNA (Ver.R7.0 with single precision) code (Fig. 3). The THUMS 3YO model was developed by Mizuno *et al.* [7]. The CRS FE model was developed based on the geometry measurements of the CRS. The Q3 dummy and human FE models seated in the CRSs were subjected to acceleration pulse based on the UN R44 test procedure. The sled acceleration pulse was defined according to the sled acceleration (see Fig. 2).

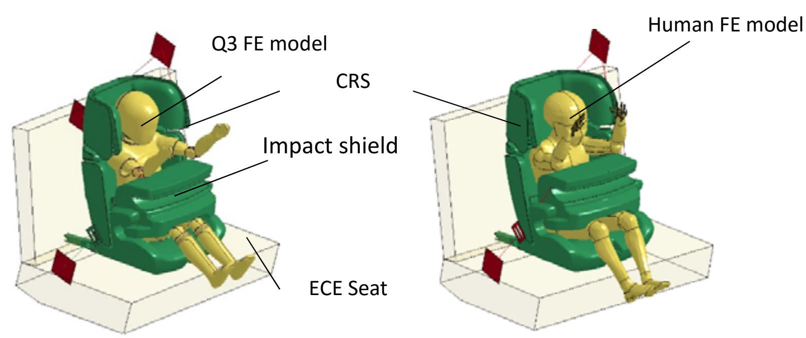

CRS B and Q3 FE model. CRS B and child human 3YO model.

Fig. 3. Impact CRS simulation set-up.

Animal test

In order to examine the internal organ injuries by an impact shield CRS, experiments using porcine were carried out for the impact shield-type CRSs (CRS A and CRS B with ISOFIX) and for the five-piont harness type (CRS C with ISOFIX and support leg). The CRS C is a convertible type CRS and therefore was also tested in the rear-facing (RF) position. The four Tibetan miniature pigs were prepared by the Laboratory Animal Centre of Southern Medical University. The Tibet miniature pig becomes an adult at the age of around 24 months (and average weight 20 kg) [16]. Since the focus of this study was on injury to 3 year-old children, 4-months old pigs were selected; 24 months * (3YO/18YO (for adult)) = 4 months, the weight of the pigs varied between 11 kg to 13 kg. The anthropometry of all pigs is listed in Table II. The body width was measured as the distance between the anterior superior iliac spines.

The test set-up is shown in Fig. 4. The pigs were seated such that the backs made contact with the CRS seatbacks. In the five-point harness CRS C FF test, the chest clip was used to connect right and left shoulder harnesses as pigs do not have shoulders and clavicles. The acceleration of the sled for each test using a pig was similar to that shown in Fig. 2.

TABLE II
ANTHROPOMETRY OF THE TESTED TIBETAN MINIATURE PIGS (FF: FORWARD-FACING, RF: REAR-FACING)

Test No.	CRS model.	Pig ID	Weight (kg)	Stature (cm)	Head Length (cm)	Abdominal perimeter (cm)	Chest circum -ference (cm)	Body Width (cm)	Sternal Length (cm)	Right Upper limb length (cm)	Right lower limb length (cm)
TC 01	CRS A	151105	13	56	17.5	69	55	11.5	13	29	36.5
TC 02	CRS B	150442	13	61	21	58.5	49.5	16	15	30.5	36.5
TC 03	CRS C FF	150807	11	54	17	54.5	51	11	12.5	27	32
TC 04	CRS C RF	151106	11.8	56	17.5	62	53	9	13.5	29.5	36

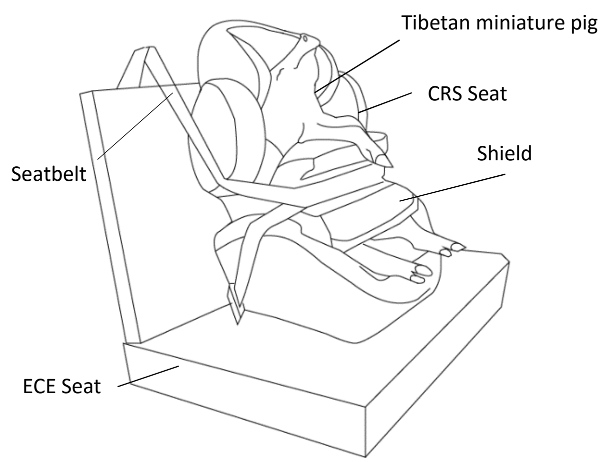

Fig. 4. Porcine test set-up.

The experiments using pigs were conducted following the recommendations of the *Guide for the Care and Use of Laboratory Animals of the National Institutes of Health*. The animal use protocol was reviewed and approved by the Institutional Animal Care and Use Committee (IACUC) of Southern Medical University, China. All efforts were made to minimise the number of animals used and their suffering. At the end of the study, all pigs were taken out of the laboratory by Laboratory Animal Centre of Southern Medical University.

Before the tests, the pigs were anaesthetised with 3% sodium pentobarbital (1 ml/kg) with normal respiration. After anaesthesia, the pigs were moved from a simple operation platform to the prepared seat and then placed as a child would be seated in the CRSs. The frontal impact tests of CRS were conducted using the UN R44 test conditions. The velocity change of the sled was 50 km/h.

During impacts, the physical parameters of the sled test (sled acceleration, impact speed) were recorded together with damage to the CRS. After the tests, the pigs were moved out of the CRSs and the respiratory rate, heart rate, corneal reflex, time of death, and symptoms were monitored. The pigs that survived the sled test were euthanised with an overdose of sodium pentobarbital two hours after impact. Then fluoroscopy and autopsy were performed for each pig, as well as the histological sections of the lung to identify any lung contusions. A 20 cm midline incision from the xiphoid to the navel was made, and all organs in the thorax and abdomen were examined carefully. Then a 5 cm anterior cervical midline incision was made at the C1-C3 level to expose the dura of the atlanto-occipital joint, and another 1 cm midline incision was made on the dura to investigate a possible spine cord or brain haemorrhage.

The injury location, abbreviated injury scale (AIS), and injury severity score (ISS) were determined for all pigs used in the study [17]. Following AIS-98 (Abbreviated Injury Scale), the ISS score (Injury severity score) was calculated as the sum of the square of the scores of AIS for the three most severely injured areas.

III. RESULTS

Dummy Tests

The kinematics of the Q3 dummy are shown in Fig. 5. The Q3 dummy exhibited flexion behaviour around the shield. The head of the Q3 made contact with the top of the shield. For the impact shield CRSs (CRS A and B), though the bottom of the CRS shell did not move from the ISOFIX attachment, the seatback moved forward. For the CRS A, the seatbelt twisted and scrunched up at the right-hand belt guide, and thereby the seatbelt movement stopped at the right-hand belt guide of the shield. As a result, the CRS rotated in the right-hand-side direction about the vertical axis. For the five-point harness forward facing CRS C, the movement of the CRS was stopped by the ISOFIX and the rotation of the CRS shell was prevented by the support leg, resulting in the forward displacement of the CRS being small. Thus, the head excursion was small and less than the injury threshold of 500 mm.

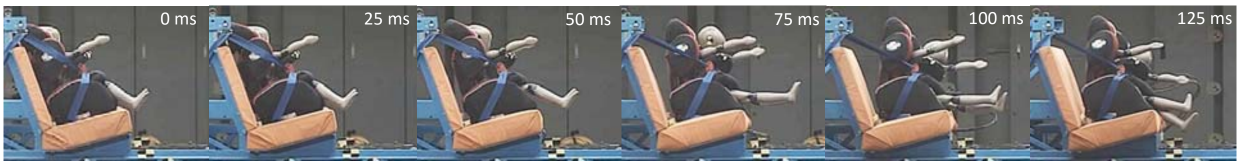

(a) CRS A

(b) CRS B

(c) CRS C FF

Fig. 5. The kinematic behaviour of Q3 in various types of CRSs (100 ms).

The time histories of chest deflection and chest acceleration are shown in Fig. 6. The chest deflections for the impact shield CRS were large since the chest was directly loaded by the shield. On the other hand, the chest deflection for the five-point harness CRS was lower compared to that in the tests using the impact shield CRSs. As the chest accelerations exhibited many “spikes”, the chest loading was difficult to evaluate from the chest acceleration (Fig. 6(b)). Table III presents the chest deflection and the chest acceleration (3 ms). The chest deflection for the impact shield CRS was between 33.6 mm and 37.5 mm. For all tests, the chest deflection was less than the proposed IARV of 40 mm. The chest acceleration (at 3 ms) was between 319.4 and 341.7 m/s^2—also below the IARV of 539 m/s^2 specified for Q3 dummy in UN R129. Thus, in the tests using the impact shield CRSs, the loads acting on the Q3 chest were less than the injury threshold.

Three reasons can be considered for large chest deflection for the CRS A. First, the seatbelt twisted and stopped going through the seat belt guide on the right-hand side of the shield (Fig. 5 (a)). This led to a sudden stop of the CRS shell, which could have resulted in a large loading on the chest. Secondly, the shape of the shield that faces against the chest is relatively flat in the CRS A as compared to CRS B. This could lead to large chest deflection of the Q3 chest. Thirdly, the forward motion of the Q3 dummy lower limbs was largest for the CRS A. This was because the shield of CRS A did not cover the pelvic area, thereby the pelvis was not restrained. The forward motion of the unrestrained pelvis and lower limbs caused a greater force transmitted to the chest. This could result in a large chest compression against the shield. The chest deflection for the five-point harness was small (20.2 mm). The harness went through the clavicles to the pelvis, and the harness loading acted on the clavicles without compressing the centre line of the rib cage (sternum). This could lead to the small chest deflection for the five-point harness CRS.

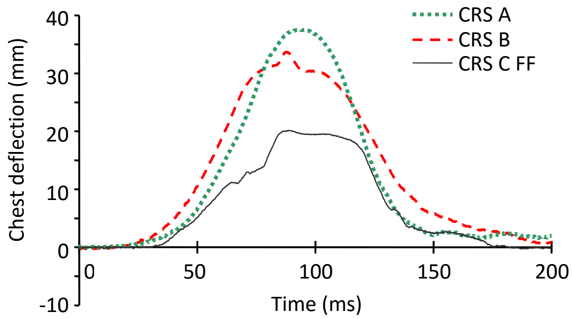

(a) Chest deflection.

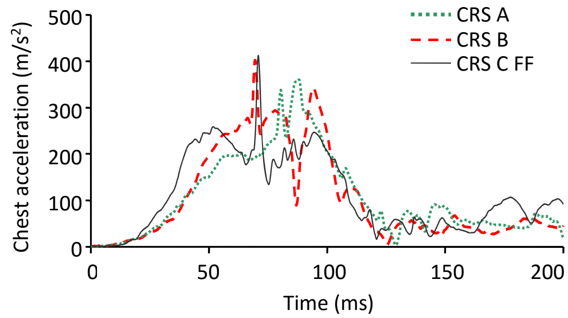

(b) Chest resultant acceleration.

Fig.6. Chest deflections and resultant accelerations of occupants in CRSs.

TABLE III
CRS Q3 DUMMY TEST RESULTS

Test No.	CRS model.	HIC15	Head acceleration (3 ms)	Chest deflection	Chest acceleration (3 ms)
D001	CRS A	151.4	400.0 m/s2	37.5 mm	341.7 m/s2
D002	CRS B	291.2	599.9 m/s2	33.6 mm	319.4 m/s2
D003	CRS C FF	133.5	410.8 m/s2	20.2 mm	253.4 m/s2

FE Simulations

Occupant kinematics

The kinematics of the Q3 dummy and THUMS 3YO child FE model obtained from the simulations for impact shield CRS B are shown in Fig.7. The Q3 dummy behavior in the FE analysis was comparable with that in the experiment (see Fig. 6(b)). For the Q3 FE model, the whole dummy initially moves forward. Then the chest makes contact with the shield, which prevents the chest from continuing to move forward. The contact area with the shield is in the lower part of the Q3 rib cage and the upper part of the pelvis. The head-neck complex underwent flexion such that the chin contacted the top surface of the impact shield. At the time of this contact, the shield deformation reached its maximum. The Q3 dummy started to lift up from the CRS at 125 ms. In contrast, the torso of the THUMS 3YO FE model wrapped around the impact shield and the whole spine continued to bend until the head impacted the top surface of the shield. Forward displacement of the pelvis was larger than for Q3 dummy, and its maximum occurred later. This was most likely caused by the relatively small size of pelvis in THUMS 3YO FE model.

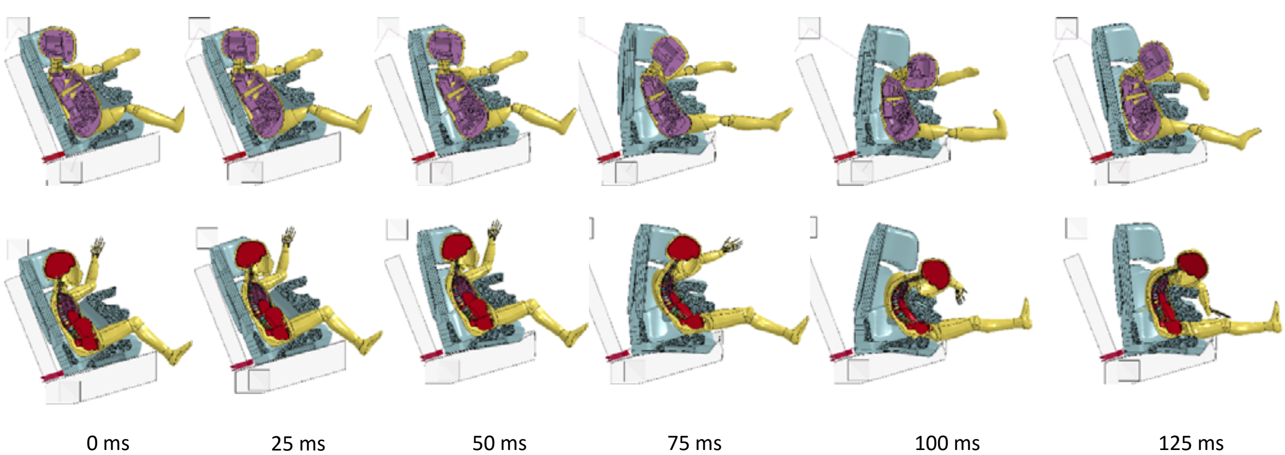

Fig. 7. Q3 and THUMS 3YO kinematics in impact shield CRS B simulations.

Injury Criteria

The chest deflection and chest acceleration of the Q3 and child FE model in the impact shield CRS B simulations are shown in Fig. 8. The chest deflection of the Q3 dummy FE model was close to that observed in the experiments using Q3 dummy. From the simulation, it is shown that the peak chest acceleration of Q3 dummy at 95 ms was caused by the chin contact with the bottom of the neck through rib cage. The chest deflection of 51 mm predicted by THUMS 3YO model was much larger and exceeded the IARV (40 mm). The chest acceleration (458.6 m/s^2 at 3 ms) predicted by the THUMS 3YO model was also larger than that predicted using Q3 dummy model (368.6 m/s^2) and observed in the experiments using Q3 dummy. There was space between the chest of the THUMS 3YO FE model and impact shield (see Fig. 8) at the initial position, and this space caused the delay of the chest resulting in large chest deflection and acceleration as compared to the Q3 dummy. HIC15 was also larger for the THUMS 3YO model than for the Q3 dummy model and the actual Q3 dummy (see Table IV).

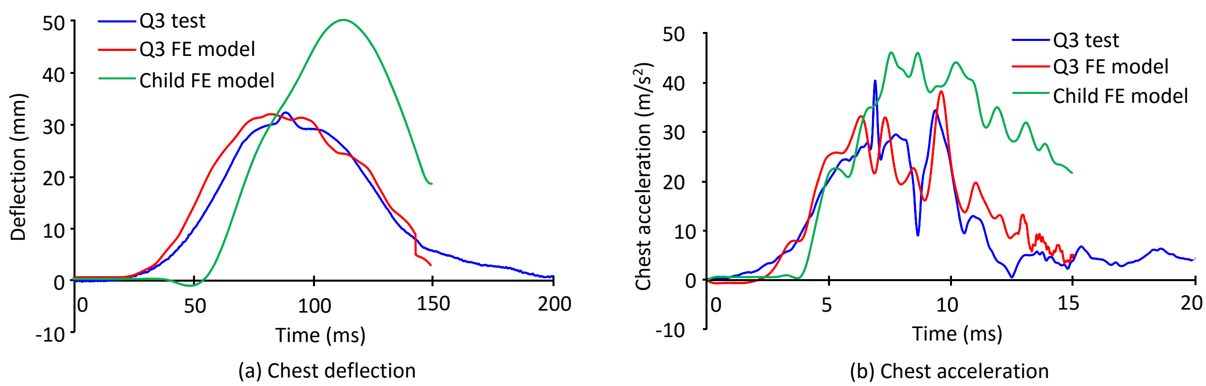

Fig.8. Chest deflection and resultant acceleration of the Q3 and child FE model for the impact shield-type CRS B

TABLE IV
CRS Q3 AND THUMS 3YO SIMULATION RESULTS FOR CRS B

Test Matrix	HIC15	Head acceleration (3 ms)	Chest deflection	Chest acceleration (3 ms)
Q3 FE model	302.6	604.7 m/s^2	32.1 mm	368.6 m/s^2
Child FE model	370	586.3 m/s^2	51 mm	458.6 m/s^2
Q3 dummy test	291.2	599.9 m/s^2	33.6 mm	319.4 m/s^2

Porcine Test

Pig Kinematic Behaviour

The pigs exhibited appreciably different kinematic responses in the experiments using impact shield CRS and five-point harness CRS. For the impact shields CRS A and CRS B, the chest and abdominal area of the pigs were directly restrained by the shield, and the torso flexion angle was large when the head forward excursion reached the maximum. In the five-point harness CRS, though the flexion angle was large, the pig was restrained in the CRS shell.

Physiological Responses and Injury Record

After the tests, the respiratory responses of the pigs restrained in the impact shield-type CRSs (CRS A and CRS B) were deep and tachypnea (Table V). The heartbeat exhibited similar behaviour. In Test 01 the pig died within 10 minutes following the test. In the rear facing CRS C (RF TC04) test, the pig survived and its respiratory responses and heartbeat were normal.

TABLE V
DESCRIPTION OF ALL PIGS AFTER IMPACT TESTING

Test No.	Pig ID	CRS type	Respiratory	Heart rate	Corneal reflex	Response	Time of death
TC 01	151105	CRS A	Deep	No	Yes	Death	10 minutes after impact
TC 02	150442	CRS B	Tachypnea	Tachycardia	Yes	Hyperspasmia	Euthanised two hours after impact
TC 03	150807	CRS C FF	Tachypnea	Tachycardia	Yes	Hyperspasmia	Euthanised two hours after impact
TC 04	151106	CRS C RF	Normal	Normal	Yes	Normal	Euthanised two hours after impact

The autopsy results, together with AIS and ISS scores, are shown in Table VI. For the pigs seated in the impact shield CRSs (CRS A and CRS B), acute subdural haematoma were observed. Resulting from a review of the video and autopsy results (see Table VI), it was determined that the flexion motion of the head-neck was large enough to pose a serious injury risk to the neck. Moreover, inner organ injuries were observed (liver laceration lung contusion, bilateral; and coronary artery laceration) despite the fact that no rib fractures occurred. The ISS score ranged from 16 to 50. This indicates that internal organ injuries could occur, even without rib fractures, for pigs seated in the impact shield CRS. In the five-point harness CRS C, though the head forward excursion was large and acute subdural haematoma were observed, the pigs were alive after the tests. It should be noticed that no injury occurred to the chest in the experiments using the five-point harness CRS C. For pigs seated in the rear-facing five-point harness CRS C, a very small acute subdural haematoma was observed. The video record showed that during the rebound phase, the restraint did not work to constrain the pig's head, leading to a complex flexion of the head-neck.

TABLE VI
AUTOPSY RESULTS WITH AIS AND ISS SCORE

Pig ID	CRS type No.	Body region	Injury (AIS score)	ISS score
151105	CRS A	Neck Chest Chest	Acute subdural haematoma (5) Lung contusion, bilateral (4) Coronary artery laceration (5)	50
150442	CRS B	Neck Chest Abdomen	Acute subdural hematoma (5) Lung contusion, bilateral (4) Liver laceration (2)	45
150807	CRS C FF	Neck	Acute subdural haematoma (5)	25
151106	CRS C RF	Neck	Acute subdural haematoma with very little bleeding(4)	16

IV. DISCUSSION

In this study, chest injuries to child occupants seated in impact shield CRS and five-point harness CRS have been analyzed using Q3 dummy test and FE simulations. Experiments using Tibetan miniature pigs were conducted to analyze the pig's chest and abdominal injuries.

From the tests performed on the Q3 dummy, the chest deflection proved large in the impact shield CRS, though it was less than the IARV (40 mm). These values were smaller than those in Tanaka's study in 2009. It is likely that the impact shield CRS was modified and designed to mitigate the loading on the chest. The chest deflection for the five-point harness FF CRS was small because the clavicles were constrained with the torso restraint. In the tests using Q3 dummy, only one test was conducted for each CRS model. Therefore, the repeatability of the Q3 dummy test results should be evaluated in future studies.

There was a significant difference between the kinematic responses and chest deflections of the Q3 dummy FE model and the child human FE (THUMS 3YO) model. Spine stiffness could be an important factor influencing these responses. In the Q3 FE model, the spine was defined as a rigid body, did not deform, and its rear to forward motion combined with the upward motion occurred during the rebound phase. The Q3 FE model rebound phase occurred earlier than for the child FE model. Zhang *et al*. [10] have reported similar results for the Q3 dummy. Therefore, modification of the Q3 dummy spine stiffness is necessary to improve accuracy of CRS performance evaluation.

Even though the chest deflection of the Q3 dummy was less than the IARV, chest and abdominal injuries were observed to have occurred in the porcine tests. In the tests using impact shields CRS A and CRS B, the most common injury to the chest was lung contusion. The lung injuries were caused by the shield during the loading phase. For two pigs, liver lacerations were found at the point where the falciform ligament attaches to the liver. The laceration was located just under the sternum, where no protection is afforded by the rib cage. The cause of this liver laceration may be the CRS shield making direct contact with the abdomen during the impact. Another possible mechanism of this injury could be that the liver may move downward during the chest compression and the falciform ligament tensed from which the liver laceration occurred. Moreover, a laceration injury of the coronary artery was observed in one of the tests using CRS A. In the porcine tests using five-point harness FF and RF, no injuries to the chest or the abdomen were observed.

From the chest deflection and chest acceleration observed in the experiments using Q3 dummy, it can be concluded that the loading acting on the chest was largest for CRS A and smallest for CRS C. This was also the case in the experiments using the pigs. Despite the fact that the Q3 dummy responses were below the IARV thresholds, injuries were observed in the porcine tests. Therefore, it appears that IARV for the Q3 dummy chest needs to be examined in the future.

In the porcine tests, the most common injury was acute subdural haematoma. The high-speed video showed that during the impact the cervical spine of the pig exhibited hyperflexion and then hyperextension. As the compression of the medulla oblongata by a blood clot was determined to be the cause of death and hyperspasmia symptoms were present, a rupture of the spinal vessels can be hypothesized. Obviously, the vessels in the spinal canal were broken during the impact, and the hyperspasmia symptom and the cause of death was the medulla oblongata being compressed by a blood clot. It is necessary to consider the anatomical differences between humans and pigs when assessing the injury outcomes of pigs. The pig has a long head and thick neck, and the face of the pig was initially directed upwards, which made the kinematics of head-neck very complex. The child finite element model predicted the contact with the shield top or the sternum constrained the neck flexion. No such contact occurred in the experiments using pigs, which led to a large flexion of the pig neck.

In addition, the heavy head and neck complex and the short limbs of the pig led to different loading on the chest. However, the torso of the pig was directly loaded by the shield, and injuries to the chest occurred. In the porcine tests, lung contusion and liver laceration injuries were found only in the shield-type CRSs. This suggests that the loading on the chest and abdominal area by the shield during the impact may cause these kind of injuries even without rib fractures.

Limitations

In the current study, only a small number of tests using pigs was performed. Moreover, given the differences in anatomy and body mass/inertia between humans and pigs, caution is required when drawing conclusions regarding the injury risk and mechanisms in human based on the responses observed in the experiments using pigs.

V. CONCLUSIONS

In this study, Q3 dummy tests, FE analyses and porcine tests were carried out to investigate the chest loading of the child occupant in the impact shield CRS and the 5-point harness CRS. The conclusions are summarized as:

i. In Q3 dummy tests conducted according to UN R44 test protocol, deflection of the Q3 dummy chest was less than the proposed injury threshold (40 mm) for the impact shield CRSs. The chest deflection for five-point harness CRS was substantially smaller compared to those observed for impact shield CRSs.

ii. In the simulations, the torso of the Q3 dummy was stiffer than that of the child FE model (THUMS 3YO), causing the Q3 dummy easier upward motion in the rebound phase. The THUMS 3YO FE model predicted large chest deflection (compression) due to the contact with the impact shield.

iii. The porcine tests showed that inner organ injuries can occur without rib fracture. Liver lacerations and bilateral lung contusions were the most common injuries observed when testing with the impact shield CRSs.

VI. ACKNOWLEDGEMENTS

The authors would like to acknowledge support of the National Natural Science Foundation of China (Project No: 31300784), the Natural Science Foundation of Fujian Province, China (Project No: 2016J01748), the high-end Foreign Experts Recruitment Program (GDT20143600027) and the Outstanding Youth Scientific Research Program of Fujian Province, China. The authors would also like to thank Prof. Hongwu Huang for his support and Prof. Adam Wittek for his valuable advice.

VII. REFERENCES

[1] Kahane C. An evaluation of child passenger safety: the effectiveness and benefits of safety seats, National Highway Traffic Safety Administration, DOT HS 806 890, 1986.

[2] Arbogast KB, Durbin DR, Cornejo RA, Kallan MJ, Winston FK, An evaluation of the effectiveness of forward facing child restraint systems, Accident Analysis and Prevention, 36(4), 585-589, 2004.

[3] Melvin W, Weber K. Abdominal intrusion sensor for evaluating child restraint systems, SAE Paper 860370.

[4] Whitman GR, Brown KA, Cantor A, D'Aulerio LA, Eisentraut DK, Markushewski. ML. Booster-with-shield child restraint case studies', SAE Paper 973307

[5] Langwieder K, Hummel T, Finkbeiner F. Injury risks of children in cars depending on the type of restraint, Child Occupant Protection in Motor Vehicle Crashes, Willey, 1999.

[6] Tanaka Y, Yonezawa H, Hosokawa N, Matsui Y, Mizuno K, Yoshida R. Responses of Hybrid III 3YO and Q3 Dummies in Various CRSs Tested Using ECE R44 Impact Conditions, ESV conference 2009.

[7] Mizuno K, Iwata K, Deguchi T, Ikami T, Kubota M. Development of a three-year-old child FE model, Traffic Injury Prevention, 6(4), 361-371, 2005.

[8] GRSP, Expert of France. Proposal for supplement 7 to the 04 series of amendments, Informal document GRSP-52-12, 52nd GRSP, 11-14 December 2012, http://www.unece.org/trans/main/wp29/wp29wgs/wp29grsp/grspinf52.html

[9] GRSP, Expert of France. A study on shield systems, Informal document GRSP-55-39, 55th GRSP, 19-23 May 2013, http://www.unece.org/trans/main/wp29/wp29wgs/wp29grsp/grspinf55.html

[10] Zhang X, Lawall C, Klimitsch C, Thurn C. Research on the difference of child anthropomorphic test device and human model in child restraint systems, 12th International Conference Protection of children in cars, Munich, Germany, December 4-5, 2014.

[11] Kent R, Lessley D, Sherwood C. Thoracic response to dynamic, non-impact loading from a hub, distributed belt, diagonal belt, and double diagonal belts, Stapp Car Crash Journal, 495-519, 2004.

[12] Mertz HJ, Prasad P, Irwin AL. Injury risk curves for children and adults in frontal and rear collisions, 41st Stapp Car Crash Conference, SAE 973318, November 1997.

[13] EEVC (European Enhanced Vehicle-safety Committee). Q-dummies report, advanced child dummies and injury criteria for frontal impact, Working Group 12 and 18 report, Document No. 514, April 2008.

[14] GRSP, Expert of France. Proposal for amendments to ECE/TRANS/WP.29/GRSP/2014/28, Informal document GRSP-55-08, 56th GRSP, 9-12 December 2014, http://www.unece.org/trans/main/wp29/wp29wgs/wp29grsp/grspinf56.html

[15] Crandall, J.R., Myers, B.S., Meaney, D.F., Zellers, S.S., Pediatric Injury Biomechanics, Chapter 3, Springer, 2013.

[16] "Tibetan Pig" Internet: [http://agtr.ilri.cgiar.org/index.php?option=com_content&view=article&id=149&Itemid=165], May 12th, 2016 [Accessed on May 12th, 2016].

[17] Wong, E. Abbreviated Injury Scale. Springer New York, 2011.